

On the seismic behavior of a reinforced concrete building with masonry infills collapsed during the 2009 L'Aquila earthquake

Michele Palermo^{*1}, Ricardo Rafael Hernandez², Silvia Mazzoni³
and Tomaso Trombetti¹

¹Università di Bologna, Viale del Risorgimento 2, 40136 Bologna, Italy

²Degenkolb Engineers, 300 South Grand Ave, Suite 1115, Los Angeles, CA, 90071, USA

³Degenkolb Engineers, 235 Montgomery Street, Suite 500, San Francisco, CA 94104, USA

(Received April 6, 2013, Revised August 20, 2013, Accepted September 22, 2013)

Abstract. The 2009 L'Aquila, Italy earthquake shook a high density area causing a wide spectrum of damage to reinforced concrete with infill buildings, one of the most common building types used in Italy. The earthquake has proven to be a "full-scale" laboratory to further understand building performance. This paper presents the first results of a joint research effort between the University of Bologna and Degenkolb Engineers, aimed at investigating the seismic behavior of an infilled frame building that collapsed during the earthquake. State-of-the-practice techniques were implemented as a way to determine the reliability of these modeling techniques in anticipating the observed building performance. The main results indicate that: (i) the state-of-the-practice techniques are able to predict the observed behavior of the buildings; (ii) the masonry infills have a great influence on the behavior of the building in terms of stiffness, strength and global ductility.

Keywords: seismic response; masonry infills; L'Aquila earthquake

1. Introduction

On April 6, 2009 at 01:32:39 UTC (03:32:39 local time), a magnitude $M_I=5.8$ ($M_w=6.3$) earthquake struck a populated area in the Abruzzo region (central Italy). The epicenter was located within 10 km of the urban center of L'Aquila, capital of the region with approximately 70,000 inhabitants. The earthquake was the third strongest recorded in Italy in the last 50 years after the 1976 Friuli ($M_w=6.4$) and the 1980 Irpinia ($M_w=6.9$). Further, it is the strongest event providing strong motion records from accelerometer stations located very close to the epicenter (approximately 4-6 km, Bursi *et al.* 2009).

The earthquake caused a total of 305 deaths and 1,500 injuries, destroyed or damaged an estimated 10,000-15,000 buildings, prompted the temporary evacuation of 70,000-80,000 residents, and left more than 24,000 homeless. The building damage extended over an area of approximately 600 square kilometers, including the urban center of L'Aquila and several villages of the middle Aterno Valley (approximately 5-10 km to the epicenter, ERII Special Earthquake Report 2009).

*Corresponding author, Ph.D., E-mail: michele.palermo7@unibo.it

A joint research work between University of Bologna and Degenkolb Engineers has been carried out in order to study a complex of seven reinforced concrete with masonry infills buildings located in Pettino (an area located in the northwest urban center), that arose a great interest in the seismic engineering community. Although the seven buildings were built in the mid-1980s adopting similar structural systems, they exhibited very different responses to the earthquake: two collapsed while the remaining five had moderate to heavy damage.

Methods for the evaluation of the seismic response of existing building have been proposed since the 1980s (fib Bulletin 24 2003). The most recent international building codes for the seismic assessment and retrofitting of existing buildings (ASCE 41 and Eurocode 8) suggest approaches based on the introduction of specific limit states and knowledge factor (or confidence factor) accounting for the uncertainty related to the knowledge of the structure. Typically, three different values of the knowledge factor are admitted indicating whether the level of knowledge is "minimum," "usual," or "comprehensive". As far as the method of analysis is concerned, nonlinear procedures, such as non linear incremental static analyses, e.g. pushover analyses (Chopra and Goel 2002) or non-linear incremental dynamic analyses (Vamvatisikos and Cornell 2002) are generally adopted rather than linear approaches (such as linear static analysis or response spectrum analysis), commonly adopted for the design of new buildings. A detailed benchmark for the modeling of existing reinforced concrete frame building can be found in a PEER report (Haselton *et al.* 2007). Performance is quantified in terms of economic losses and collapse safety. The assessment includes site-specific seismic hazard analyses, nonlinear dynamic structural response simulations to collapse, damage analyses, and loss estimation. Guidelines for the case of old reinforced buildings designed prior modern seismic design requirements can be found in Manfredi *et al.* 2007. In the case of absence of original drawings and lack of information the fundamental phase of the methodology proposed by Manfredi *et al.* lies in the application of the procedure called "Progetto Simulato" aimed at reconstructing the most probable geometrical and mechanical building details applying the state-of-the-art at the construction time of the building. An application of the Eurocode 8 procedures to an infilled reinforced concrete is detailed in Tanganelli *et al.* 2013.

The objective of the overall research work is to investigate the possible reasons that caused the observed responses. In detail, the present paper presents the first results of the research specifically focused on the study of one of the two collapsed buildings with the main purpose of developing a model able to reproduce the seismic response of the collapsed building. This paper presents an interpretation of possible causes leading to different seismic responses of the seven buildings. Analyses have been conducted according to the ASCE 41 for the modeling features and following the prescription of old Italian building codes for the determination of the material properties.

2. Observed damage of RC buildings

The building damage observed from the L'Aquila earthquake varied substantially depending on the building type, distance from the epicenter, age of construction, condition of the structure. In some locations, there was also evidence of local soil amplification effects (ERII Special Earthquake Report 2009).

The mainshock caused heavy building damage in the center of L'Aquila, where MCS (Mercalli-Cancani-Sieberg) intensity varied between VIII and IX. Building damage was even more significant in some villages located in the middle Aterno Valley where intensities as high as IX-X

were experienced in Castelnuovo and Onna (Table 1, from Galli *et al.* 2009). The effects of soil amplification with high level of damage (VIII) and some collapsed buildings were observed in Pettino, an area located in the northwest area of the center of the city. Fig. 1 shows the distribution of the MCS intensity in the area struck by the earthquake (available on INGV web site, <http://www.mi.ingv.it/eq/090406/quest.html>).

Reinforced concrete buildings in the L'Aquila region performed, on average, fairly well, considering the limited seismic design requirements imposed by the Italian code prior to 2009, and the severe ground shaking, substantially higher than the original design level. The most common damage affected the exterior and interior infills varying from diagonal cracks to out-of-plane failure. However, there were also isolated cases of collapse like the Hotel Duca degli Abruzzi, the student housing observed in the historic center of L'Aquila, and 3 cases in Pettino (ERII Special Earthquake Report 2009).

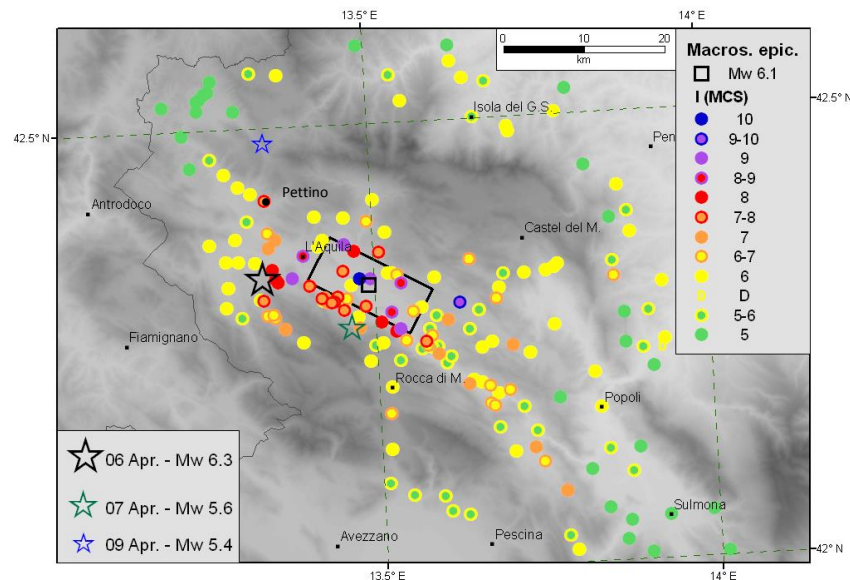


Fig. 1 Distribution of the macroseismic intensity (MCS scale), available on <http://www.mi.ingv.it/eq/090406/quest.html>

Table 1 The highest MCS intensity measure estimated after the 6 April 2009 L'Aquila earthquake in L'Aquila Province

Site	City	Lat. [°]	Long. [°]	MCS
Castelnuovo	L'Aquila	42.295	13.628	IX-X
Onna	L'Aquila	42.327	13.460	IX-X
San Gregorio	L'Aquila	42.327	13.496	IX
Sant'Eusanio	Sant'Eusanio	42.288	13.525	IX
Forconese	Forconese			
Villa S. Angelo	Villa S. Angelo	42.269	13.538	IX
L'Aquila centro	L'Aquila	42.356	13.396	XIII-IX
Paganica	L'Aquila	42.358	13.473	XIII
Pettino	L'Aquila	42.325	13.355	XIII

Among these, particular interest has been focused on one collapsed building, part of a residential complex of seven condominiums located in Via Dante Alighieri, Pettino. The seven structures are reinforced concrete with masonry infills buildings of three to four stories constructed in the mid-1980s and consisting of 6 to 9 apartments. The plan is similar for all the buildings including the presence of a porch at the ground level. Despite these similarities, the seven buildings exhibited three different levels of damage: (A) Collapse; (B) Moderate damage (i.e. Repairable); (C) Minor damage (i.e. Occupiable). Specifically, two buildings collapsed with a soft

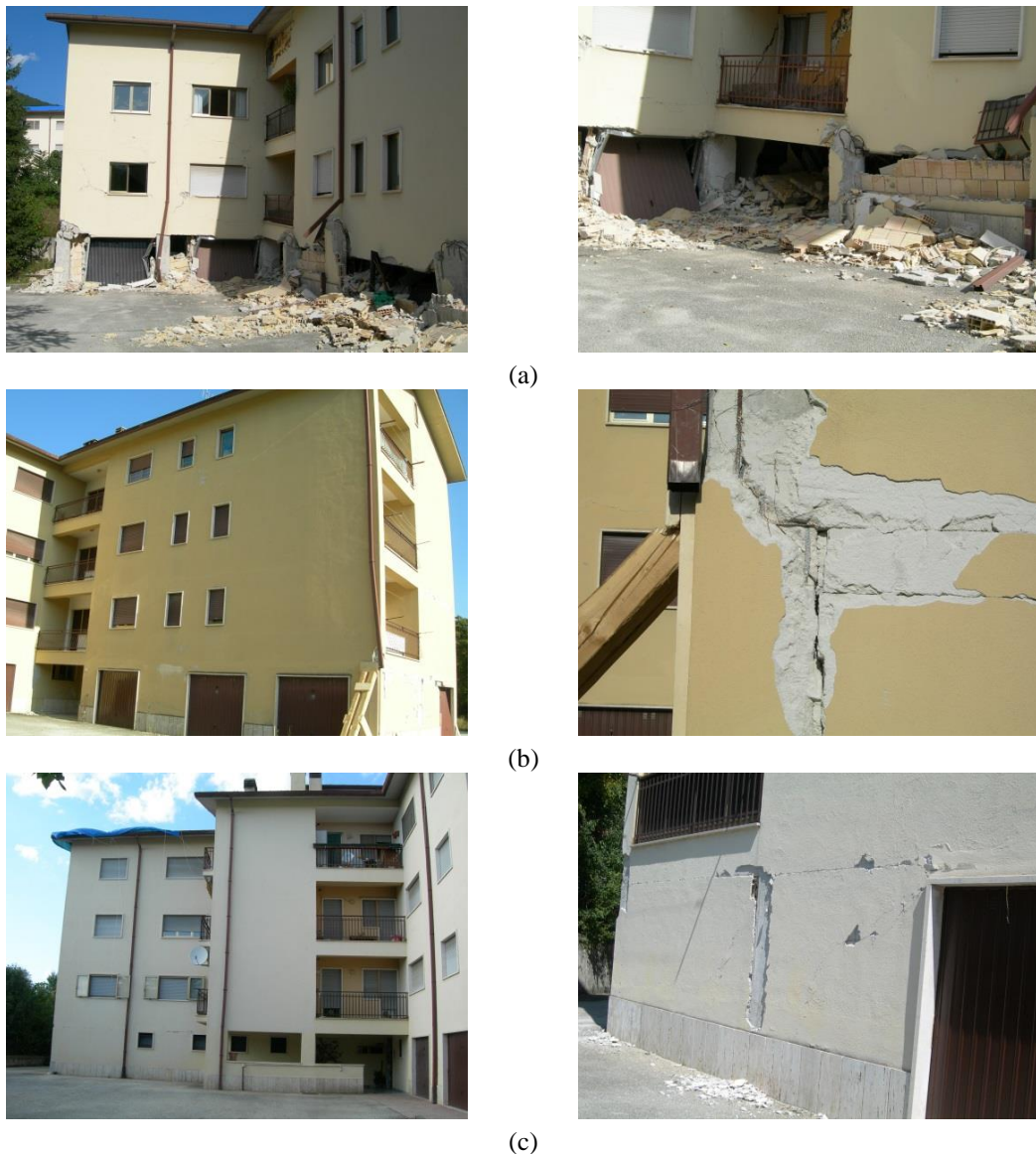


Fig. 2 Global state of damage (left) and particular of damage (right) for each of the 3 different types of damage observed: (a) Collapse, (b) Medium (Repairable) and (c) Low (Occupiable)

story mechanism at the ground level (level of damage A); two buildings had cracks on the exterior infills and damage to some perimeter columns (level of damage B); three buildings displayed damage concentrated at the lower levels of the exterior infills with cracks near the openings (level of damage C). Fig. 2 shows selected details of the damaged and collapsed buildings.

3. Case study

3.1 Building description

The studied building is one of the two buildings that collapsed in Via Dante Alighieri. It is a four-story condominium built between the late 1970s and 1980s and designed prior to modern day seismic detail requirements. According to the seismic code at the time of construction (D.M. 3/03/1975), a reinforced concrete building located in L'Aquila should be designed for a total lateral force (e.g. the base shear) equal to $F_h = C R I W$ (where $C=0.07$; $R=1.0$; $I=1.0$ and W equal to the weight of the building) and corresponding to a design spectral acceleration equal to 0.07 g.

The external dimensions in plan are 25 m (80 feet) by 28 m (90 feet). The maximum height of the building roof ridge is 12.5 m (40 feet) with the 2nd, 3rd and 4th story, respectively, at 2.8 m (9 feet), 5.8 m (19 feet) and 8.8 m (29 feet) from the ground level. It is to be noted that: (i) a portion of the first story is built as an open porch; (ii) all the garages are located in the same direction.

Fig. 3 gives the structural plans of the building. Also the column numbering is indicated.

3.2 Observed damage

Observation of the collapsed building revealed that: (i) most of the perimeter columns at the ground story failed in shear with some evident buckling of the longitudinal bars (no transverse reinforcement within the joints); (ii) the exterior infills at the ground story exhibited various failure mechanisms (some panels had evident diagonal cracks with corner crushing while others failed due to out-of-plane effects).

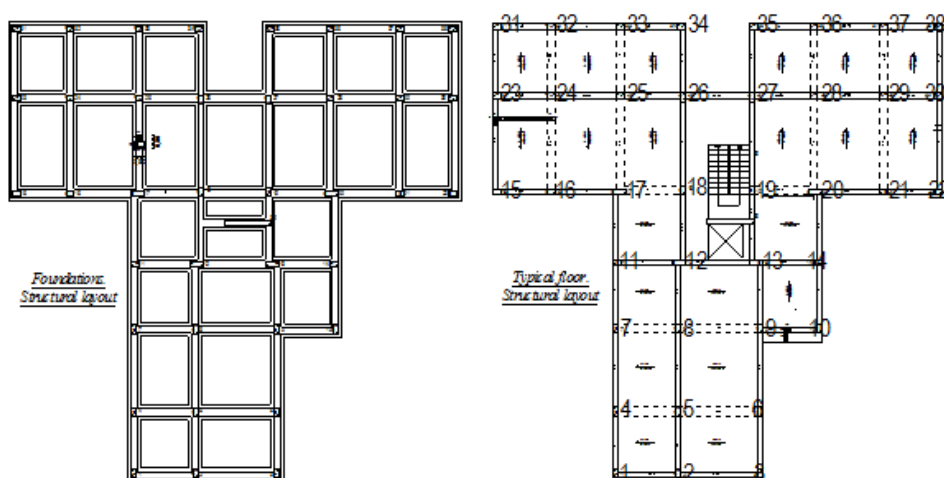


Fig. 3 Structural plans of the building: (a) Foundations and (b) Typical floor

The observed damages indicate a soft/weak story mechanism of collapse. Furthermore, it can be observed, from the particular location of the collapsed columns, that the building experienced a significant torsional response. Fig. 4 gives selected details of the observed damages.



Fig. 4 Damages observed for the studied building: (a) Soft/weak story mechanism, (b) Shear failure in columns and (c) Infills failure

3.3 Geometric and mechanical characteristics – RC frame

The geometric and mechanical properties for the structural elements were partially obtained from in-situ measurements and estimated based on the building code at the time of construction (D.M. 26/03/1980, D.M. 3/03/1975). Table 2 provides the dimension of the typical cross section

and typology and size of reinforcement for columns and beams obtained from the in-situ reconnaissance. The nominal shear strength of the typical columns (cross section of 50 x 30 cm, see Table 2), evaluated according to the Eq. (6-4) of ASCE 41, is around 150-160 kN, and the most probable expected mode of failure is shear failure (condition iii of Table 6-8 of ASCE 41).

Table 2 Cross section dimension and reinforcement details for columns and beams

Structural element	Cross section [cm x cm]	Longitudinal bars [mm]	Ties** [mm]	ρ_L *** [%]	ρ_T *** [%]
Exterior columns	50 x 30*	deformed - ϕ 16	smooth - ϕ 8@ 15-20 cm	1.0	0.5-0.7
Interior columns	50 x 30*	deformed - ϕ 16	smooth - ϕ 8@ 15-20 cm	1.0	0.5 0.7
Exterior beams	50 x 30	deformed - ϕ 16	smooth - ϕ 8@ 15-20 cm	1.0	0.5 0.7
Interior beams	50 x 30 / 20 x 50	deformed - ϕ 16	ϕ 8@ 15-20 cm	1.0 / 1.6	0.5 / 1.0

* Two columns have a cross section of 80 cm X 80 cm.

** Spacing at column boundaries. Spacing at mid-section is approximately 30 cm.

*** ρ_L and ρ_T are the longitudinal and transversal reinforcement ratios, respectively.

The mean compressive strength of the concrete was measured in situ and resulted equal to 20 MPa. Other mechanical properties of the RC elements, which could not be determined experimentally, (i.e. the steel strength/modulus) were evaluated following the suggestions reported in De Stefano et al. (2013) and the specifications and prescriptions of the Italian code at the time of the construction (D.M. 26/03/1980, D.M. 3/03/1975).

3.4 Geometric and mechanical characteristics – infill

The geometric properties of the exterior and interior infills were directly measured in-situ. The exterior walls consist of a double wythe brick infill, specifically a 10 cm air gap between 12 cm and 8 cm wide brick infill. The interior walls are a single layer of 8 cm wide brick. The bricks are hollow with approximately 60 percent of voids.

The mechanical properties assumed for the masonry are taken from the results of experimental tests performed in L'Aquila on masonry with age and construction similar to the case study (Colangelo 2005) and are summarized in Table 3.

Table 3 Geometrical and mechanical properties of the exterior and interior infills masonry

Element	Masonry total thickness*[cm]	Brick dimension [cm x cm x cm]	Number of layers	E_m ** [MPa]	f_v *** [MPa]
Exterior Infill	34	24x24x12	2 masonry + 1 air	3200	0.35
Interior Infill	8	24x24x8	1 masonry	3200	0.35

* total thickness including the middle air gap

** Masonry elastic modulus

*** Masonry shear strength

4. Accelerograms at the site for the studied building

The mainshock has been recorded by 57 stations belonging to the RAN (National Accelerometric Network). In this paper the accelerograms recorded by four stations (AQA, AQV, AQG, AQK), located at a distance less than 6 km from the epicenter (Mausi and Chiausi 2009, Iervolino and Chioccarelli 2010, Chioccarelli *et al.* 2009), have been used to perform the analysis. The case study building is approximately 5 km from the epicenter (Fig. 5). Details of these four selected records are given in Table 4.

Table 4 Selected strong motion station with site coordinate, soil type classification (NTC-2008), epicentral distance and PGA recorded

Code	Name	Lat. [°]	Long. [°]	Soil type	Epicentral Distance [Km]	Recorded PGA [g]
AQV	V. TERNO-CENTRO VALLE	42.377	13.344	B	4.8	0.66
AQA	V. ATERNO-F. TERNO	42.376	13.339	B	4.6	0.44
AQG	V. ATERNO-COLLE GRILLI	42.373	13.337	B	4.4	0.48
AQK	AQUIL PARKING	42.345	13.401	C	5.6	0.36

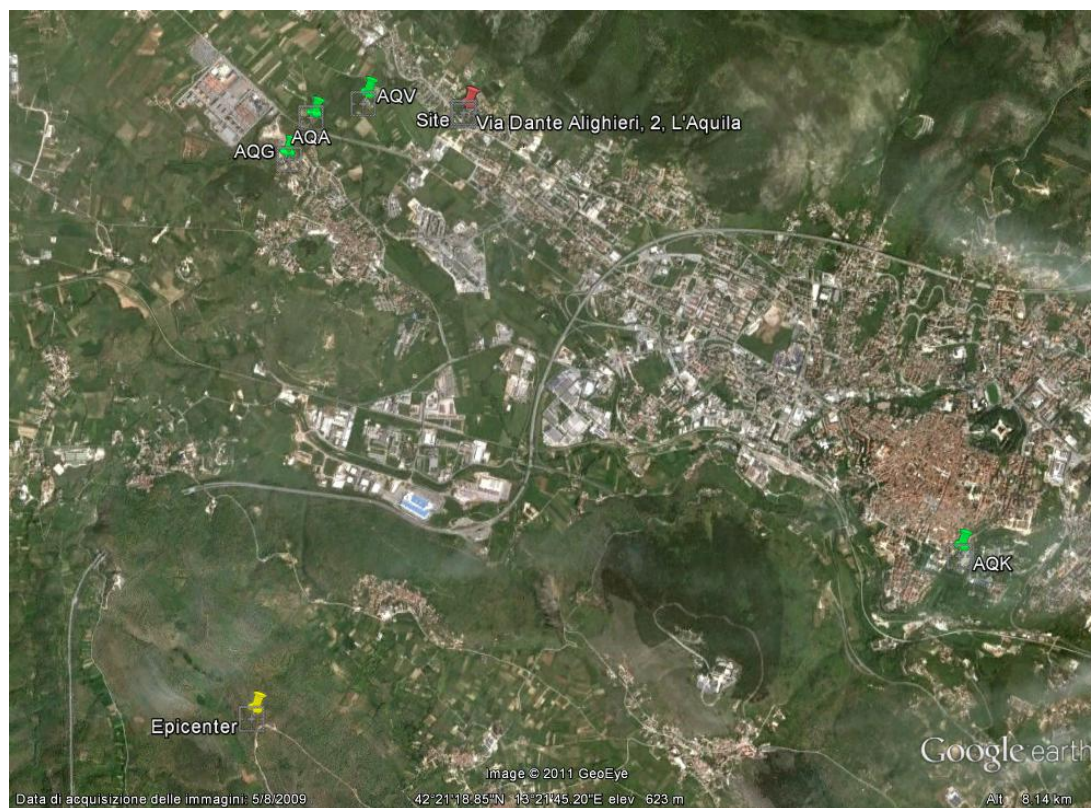


Fig. 5 Location of the epicenter (marked in yellow), strong motion stations (marked in green) and site of the building (marked in red); Google Earth

The four accelerograms recorded by the selected stations were used to obtain an estimation of the base acceleration experienced by the building.

For each record, as obtained at the k -th station, the corresponding PGA (referred to as PGA_k) was extrapolated. Then, accounting for the soil characteristic through a soil amplification factor (referred to as AF_k), the PGA at bedrock condition (referred to as PGA_k^B) was estimated by dividing the PGA_k by the soil amplification factor AF_k . Each value of d_k (epicentral distance of the k -th station) and PGA_k^B is used to obtain an attenuation curve, assuming the Sabetta- Pugliese (Sabetta and Pugliese 1996) attenuation relationship. Using the Sabetta-Pugliese attenuation relationship, graphically represented in Fig. 6, the $PGA_{P,k}^B$ (i.e. the PGA at the building epicentral distance) has been estimated.

The mean value of the $PGA_{P,k}^B$ over the four stations provides an estimate of the PGA at the site of the building assuming a bedrock condition ($PGA_P^B = \frac{1}{4} \sum_{k=1}^4 PGA_{P,k}^B$). The resulting mean value of $PGA_{P,k}^B$ is equal to 0.408 g. Finally, multiplying $PGA_{P,k}^B$ by the soil amplification factor at the building location, AF_P (estimated equal to 1.7 from the seismic microzonation map of the L'Aquila area available on line on <http://www.protezionecivile.gov.it>), a value of PGA equal to 0.695 g ($PGA_P = \frac{1}{4} \sum_{k=1}^4 PGA_{P,k}^B \cdot FA_P = PGA_P^B \cdot FA_P = \frac{1}{4} \sum_{k=1}^4 PGA_{P,k}$) gives an estimate of the PGA experienced by the building considering the actual soil conditions.

Table 5 provides the values of d_k , PGA_k^B , $PGA_{P,k}^B$, $PGA_{P,k}$ (i.e. $PGA_{P,k}^B AF_k$) and AF_k for each station and the corresponding mean value over the four stations. It can be noted the mean values of PGA_k^B and $PGA_{P,k}^B$ are very close (0.412 and 0.408, respectively) due to small differences between the station epicentral distances and the building epicentral distance.

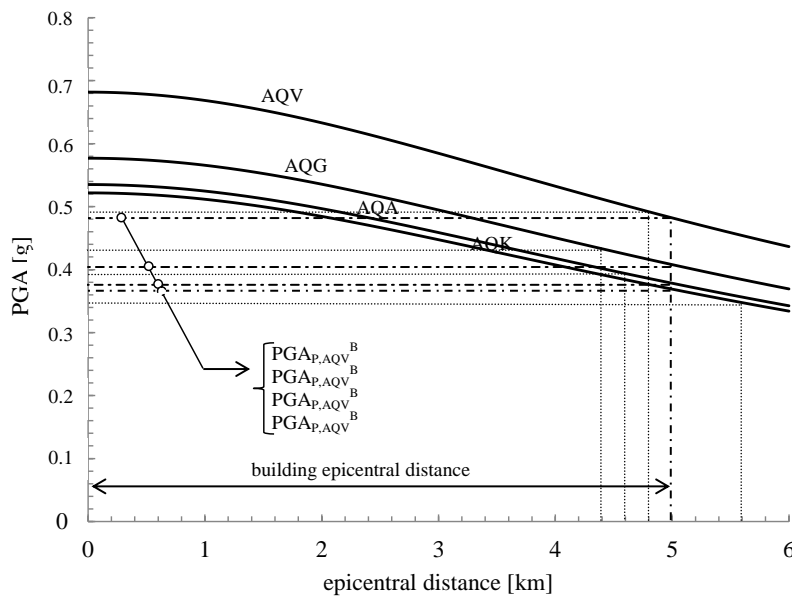


Fig. 6 Graphical representation of the procedure adopted to scale the PGA_k^B at a distance equal to the building epicentral distance in order to obtain the $PGA_{P,k}^B$

Table 5 Values of PGA_k^B , $PGA_{P,k}^B$, $PGA_{P,k}$, corresponding mean value over the four stations and amplification factor AF_k for each station

Station	Epicentral Distance, d_k [Km]	PGA_k^B [g]	$PGA_{P,k}^B$ [g]	$PGA_{P,k}$ [g]	AF_k
AQV	4.8	0.495	0.482	0.819	1.33
AQA	4.6	0.395	0.375	0.637	1.11
AQG	4.4	0.435	0.408	0.694	1.11
AQK	5.6	0.360	0.370	0.629	1.00
Mean	4.8	0.412	0.408	0.695	1.14

5. Numerical model of the building

A number of finite element models were developed using the open source software Opensees, (Mc Kenna *et al.* 2005) in order to: (i) understand the factors that contributed to the collapse of the building, (ii) determine if a prediction of failure using current analysis techniques was possible; (iii) evaluate the influence of the column seismic details (i.e. ductility) on the seismic behavior of the building.

In the following subsections, the modeling techniques adopted for columns (with particular regard for modeling the shear failure) and infills will be described. A brief description of the different building models developed in order to accomplish the proposed objectives is provided.

5.1 Column shear failure

Columns were modeled using “Beam-Column elements” (McKenna *et al.* 2005) and a fiber section to better predict the stiffness of the concrete columns and to include a consideration of the axial-flexure interaction. “Zero-length elements” (McKenna *et al.* 2005) were added at each top and bottom of columns in order to account for the mechanism of shear failure. A “zero-length element” has two nodes connected by multiple “UniaxialMaterial objects” (McKenna *et al.* 2005) placed at the same coordinate, thus leading to an element of null length. A generalized force (i.e. force or moment)-displacement (i.e. displacement or rotation) relationship allows to define the behavior of this special element. For the specific case, the adopted relation is a shear vs horizontal displacement (V-d), backbone curve. Two different backbone curves (graphically represented in Fig. 7) have been adopted for the zero-length elements:

- Brittle model;
- Semi-ductile model.

The Brittle backbone curve (Fig. 7(a)) is representative of a column expected to experience a shear mechanism (condition iii of Table 6-8 of ASCE 41). This behavior is typical of columns designed prior modern seismic requirements, as in the case of the studied buildings. With reference to the curve plotted in Fig. 7, the shear strength, V_n , is estimated per ASCE 41 considering the two contributions of concrete and transverse reinforcement. The initial stiffness of the curve is equal to the column shear stiffness:

$$K_s = \frac{A_s G}{l_c} \quad (1)$$

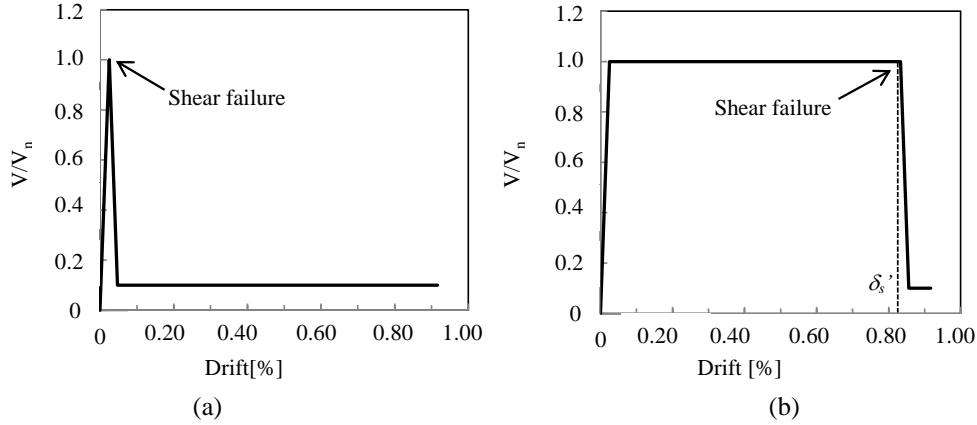


Fig. 7 Normalized backbone curves for the zero-length element placed at the top column at the bottom story: (a) Brittle model and (b) Semi-ductile model

where A_s is equal to A_g/χ (where A_g is the gross section area and χ is the shear factor equal to 1.2 for rectangular sections); G is the shear modulus of concrete and l_c is the length of the columns. A fictitious residual (a numerical artifact) strength V_{res} is assumed to be equal to $0.1V_n$

The Semi-ductile backbone curve (Fig. 7(b)) is representative of a column expected to show a flexure-shear mechanism (condition ii of Table 6-8 of ASCE 41). This behavior is typical of columns with light transverse reinforcement (Elwood and Moehle 2005). In this case the backbone curve is characterized by a post inelastic branch that follows the initial elastic behavior, indicating a ductile behavior. The ultimate drift at shear failure has been estimated according to Elwood and Moehle 2005 using the following relationship:

$$\delta_s = \frac{3}{100} + 4\rho'' - \frac{1}{40} \frac{\nu}{\sqrt{f'_c}} - \frac{1}{40} \frac{P}{A_g f'_c} \quad (2)$$

Where ρ'' is the transverse steel ratio, ν is the nominal shear stress, f'_c is the concrete compressive strength, P is the axial load on the column and A_g is the gross cross-sectional area. For a transverse steel ratio between 0.50% and 0.80% (typical at the time of construction of the studied buildings) Eq. (2) predicts values of ultimate drift between 3.0-5.0% depending on the variation of axial load due to earthquake loading. Note that in Eq. (2), δ_s represents the displacement of the total column displacement, thus in order to use that equation for the zero-length element it is necessary to subtract the flexural component of the horizontal displacement (δ_{flex}) from δ_s , leading to the following relationship for the evaluation of the ultimate drift of the zero-length elements:

$$\delta_s' = \delta_s - \delta_{flex} \quad (3)$$

Fig. 7(b) displays the Semi-ductile model adopted for the zero-length element placed in correspondence of a 50 cm X 30 cm column at the bottom story.

5.2 Infills

The infills have been modeled using nonlinear equivalent struts following the general approach proposed by Al-Chaar (Al Chaar 2002). The Al-Chaar approach to determine the properties of the equivalent strut is based on the following: (i) Evaluation of the equivalent strut width; (ii) Evaluation of the strength of the equivalent strut; (iii) Evaluation of the inelastic behavior of the strut.

The equation used to calculate the equivalent strut width, a , of a full panel is based on a conservative approach by Mainstone (Mainstone 1971) which establishes a lower bound of the expected elastic stiffness of the infill (Al Chaar 2002). Table 6 gives the value of the equivalent width, a , related to three different amount of opening in the infills. To estimate the effective infill stiffness in a more accurate way, (i.e. less conservatively) an effective masonry modulus $E_{m,eff}$ has been estimated based on experimental data from cyclic tests performed on infill panels built using the same type of brick and technology of those of the studied building (Colangelo 2005). The results of this study showed that an effective value of $E_{m,eff}$ equal to $3E_m$ was required. A qualitative comparison between the bilinearized pushover response for the model with the actual masonry stiffness E_m and the model with the effective stiffness $E_{m,eff}$ is plotted in Fig. 8.

Table 6 Calculated value for the equivalent strut width, a , for different type of opening

	Type of opening			
	No opening	Small opening (i.e. window)	Normal opening (i.e. door)	Large opening (i.e. garage)
Equivalent strut width, a [cm]	50-60	30-40	20-30	10-20

Where the values calculated are referred to the following properties of the frame/masonry infills:

$l/h = 1.2 - 2.2$ (ratio between length and height of the infill)

$t_m = 18$ cm (infill equivalent thickness)

$E_m = 3200$ MPa

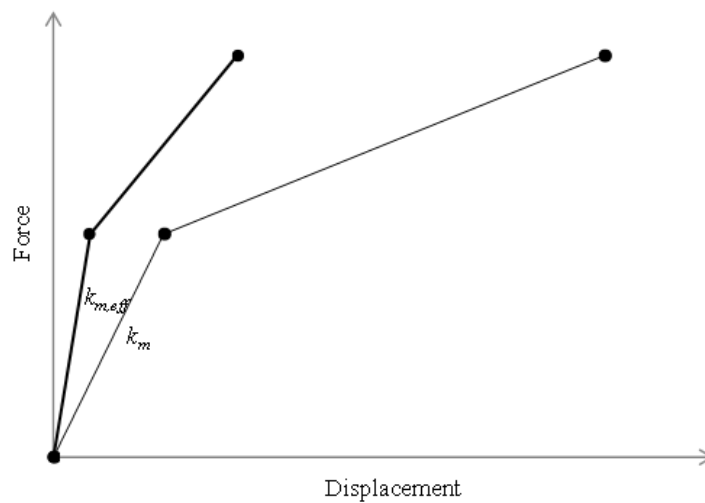


Fig. 8 Bi-linearized Push over curves for the models with the real masonry stiffness, K_m (thin line) and the effective stiffness, $K_{m,eff}$ (thick line)

The in-plane strength (R_{strut}) has been estimated as the minimum between the masonry infill crushing strength (R_{cr}) and the masonry infill shear strength (R_{shear}). The ultimate drift of the infill has been estimated per ASCE 41, which provides drift values as a function of the infill aspect ratio and the ratio of frame to infill strength (note that the range of the ultimate drifts per ASCE 41 is 0.3 % to 1.2 %). The shear mechanism of the infill occurs when the inter-story drift equals the ultimate drift. As an example, the normalized axial force vs drift relationship for a strut model of an infill panel at the bottom story is plotted in Fig. 9.

Fig. 10 provides a simple graphical representation of the single infilled frame. It can be noted that two diagonal struts (with no tensile load carrying capacity) are used to model each infill; zero-length elements are placed at the top and bottom end of each column. It is clear that the presence of diagonal struts induce concentrated shear forces at the bottom and top column nodes which may cause a brittle shear failure.

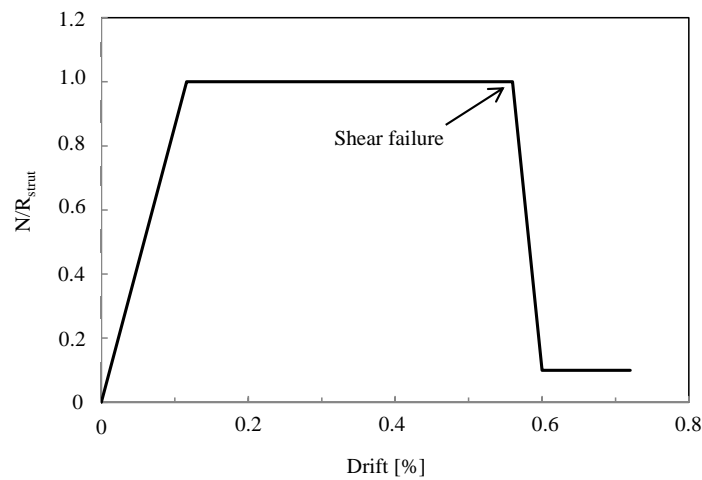


Fig. 9 Normalized axial force versus drift relationship for a strut modeling a full panel at the bottom story with a length of 5.0, height of 2.8 m and equivalent width equal to 46 cm

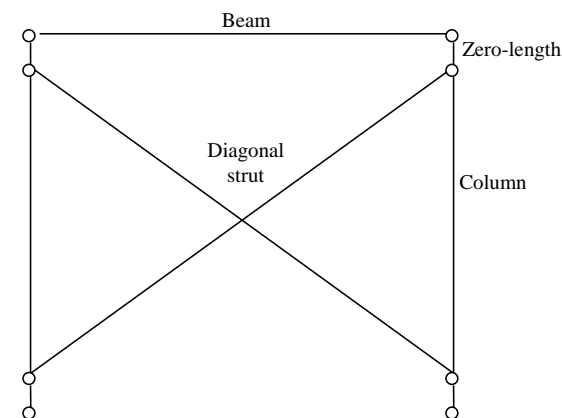


Fig. 10 Single Infilled Frame model

5.3 Building models

Three different building models have been developed with the purpose of investigating the influence of the infills and the influence of the column ductility to the seismic response of the building:

- a. Bare Frame (BF): Columns, beams and foundations were included in the Opensees (McKenna *et al.* 2005) model. The infills are not explicitly modeled; however their contribution in terms of mass was included;
- b. Infilled Frame-Brittle (IF-B): Infills are explicitly modeled as equivalent struts following the procedure described in the previous section. The backbone curve adopted to represent the column behavior in shear is the Brittle model introduced in the previous section;
- c. Infilled Frame-Semi-ductile (IF-D): Infills are explicitly modeled as equivalent struts following the procedure described in the previous section. The backbone curve adopted to represent the column behavior in shear is the Semi-ductile model introduced in the previous section.

It has to be noted that all developed models are not able to reproduce a real building collapse, (loss of axial load capacity), since no interaction between shear and axial column strength has been provided. Therefore, the terms “soft/weak story mechanism” or “collapse”, used in the section Analysis and results, will indicate the shear failure of the lateral resisting system (i.e. columns and infills).

6. Analysis and results

This section presents the main results obtained through the development of: (i) Response History Analysis; (ii) Pushover analysis; and (iii) Incremental Dynamic Analysis. These analyses were developed in order to provide meaningful simulations of what happened in the night of the 6 April 2009. In details the two main purposes are:

- Evaluation of the effect due to the presence of the exterior infills on the seismic response.
- Evaluation of the effect due to the columns ductility on the seismic response.

6.1 Response History Analysis (RHA)

The Response History Analysis (RHA) has been performed on the two infilled models (IF-B and IF-D) using the selected ground motions scaled at a value of PGA equal to 0.7 g which represents an estimate of the PGA experienced by the building during the 2009 earthquake. Although the models exhibited a similar response to the different accelerograms, for sake of brevity, only the results obtained using the AQV record will be discussed further. Specifically, the main objective is to evaluate the effect of the assumption regarding different column behavior in shear (and thus the effect of different column seismic details) on the seismic response.

Figs. 11(a) and (b) show the roof displacement response history (i.e. the response of the master node at the roof) observed for the IF-B model and IF-D model, respectively. The peak roof displacements are equal to 7.11 cm (corresponding to a roof drift equal to 0.62%) for IF-D model and 6.16 cm (corresponding to a roof drift of 0.53%), both in the x-direction (see Fig. 3 for the indication of the x and z direction), IF-B. The two responses highlight that, while IF-D

displacement response comes to zero after the end of the ground shaking, the IF-B response history exhibits a residual displacement on the x-direction equal approximately to 2 cm, indicating a failure mechanism. A more clear understanding of the different model responses is provided by the comparison of the maximum inter-story drift response history (i.e. the inter-story drift at the master node of each story, Fig. 12). IF-B interstory-drift response, represented in Fig. 12(a), shows a high drift at the first story indicating a soft/weak story mechanism, while IF-D inter-story response, represented in Fig. 12(b), shows higher drifts at the upper stories (less than the maximum value exhibited by the IF-B response at the bottom story) indicating a more uniform damage distribution along the building stories.

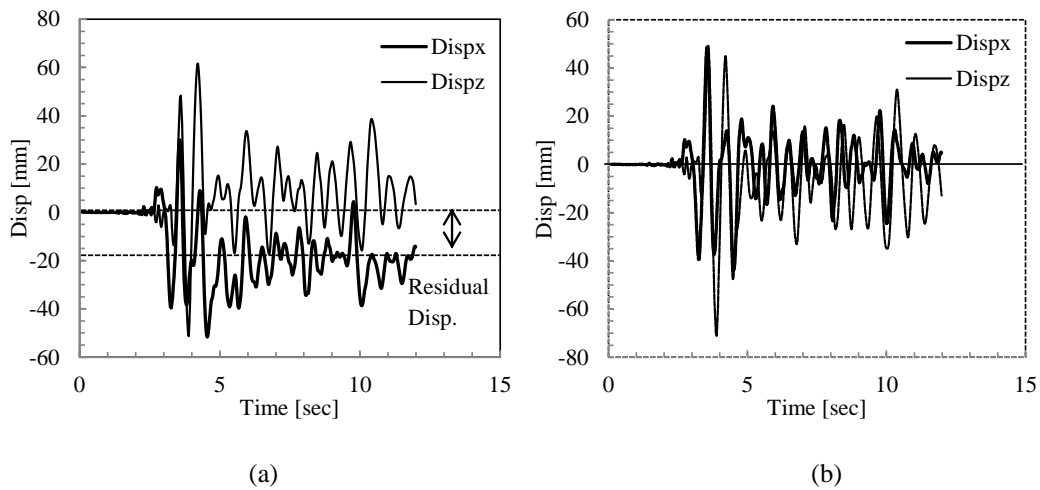


Fig. 11 Roof displacement Response History (AQV ground motion): (a) IF-B model and (b) IF-D model

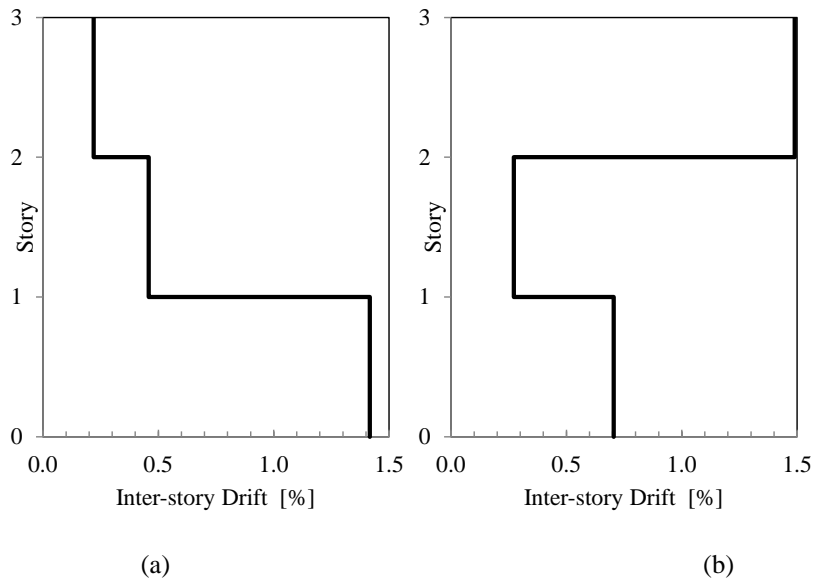


Fig. 12 Maximum interstory-drift (AQV ground motion): (a) IF-B model and (b) IF-D model

Figs. 13 graphically illustrate the envelope of the maximum first floor displacement for the IF-B model and IF-D model, respectively. The envelope represented in Fig. 13(a) reveals that the IF-B model experiences a significant torsional response due to a progressive “asymmetric” failure of the lateral resisting elements. On the contrary, the envelope of IF-D model (Fig. 13(c)) does not reveal a significant torsion of the building. Fig. 13(b) shows columns 2 and 15 after the earthquake. Figs. 14 and 15 compare the shear response history of the zero-length elements placed at the top of column 2 and the axial force in a selected strut (the one representing the infill 2) for the two models. It can be first noted that in the IF-B model the column failed in shear (i.e. the shear in the zero length elements reaches the capacity V_n and then drops to the residual strength, V_{res}), while in the IF-D model the column is able to sustain the loads for all the duration of the ground motion. Moreover it should be highlighted that in the IF-B model column 2 failed just after the failure of the related infill.

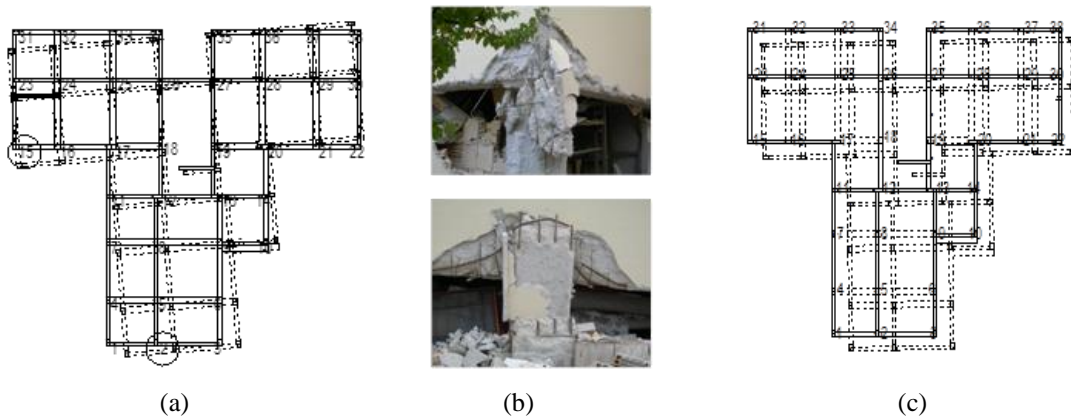


Fig. 13 (a) Torsional envelope response of the building from the RHA analysis (AQV ground motion), (b) photos of the columns marked as 2 and 15 (and circled in Fig.13(a)) after the earthquake and (c) Torsional envelope response of the IF-D model from the RHA analysis (AQV ground motion)

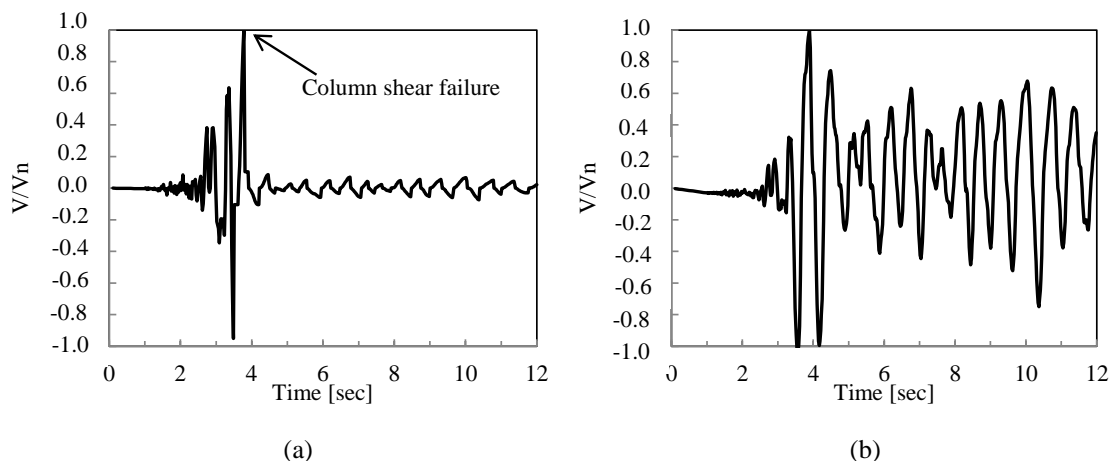


Fig. 14 Normalized Shear force Response History for the zero-length element at the bottom story for column 2: (a) IF-B model and (b) IF-D model

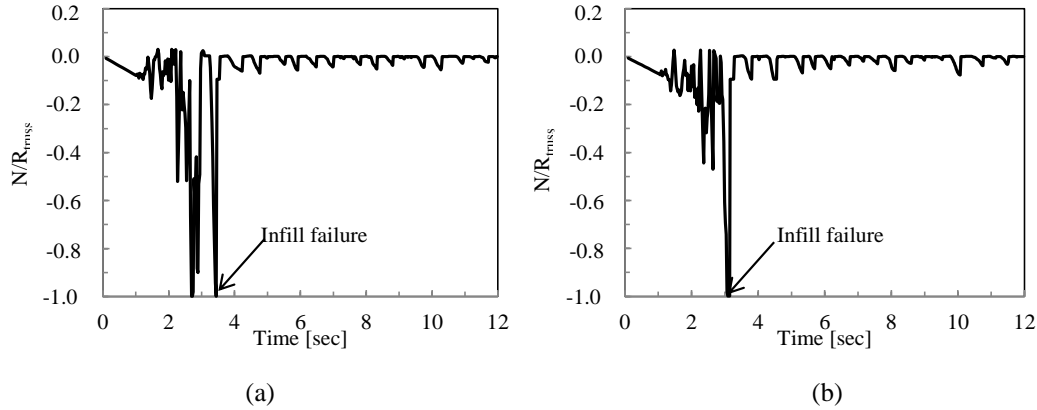


Fig. 15 Normalized Axial force Response History for strut 2 (strut 2 represents the infill between the columns indicated as 2 and 3 in Figure 4): (a) IF-B model and (b) IF-D model

Table 7 Comparison of the damages observed from the response history analysis and in situ observations of the collapsed building

Damage Type	In-situ observation	RHA	
		IF-B	IF-D
Mechanism of collapse	Soft/weak mechanism at 1 st story	Soft/weak mechanism at 1 st story	Not observed
Column shear failure	At 1 st story	At 1 st story	Not observed
Infill failure	At 1 st story	At 1 st story	At 1 st and 3 rd story

Table 7 provides a qualitative comparison of the damage obtained from the response history analysis and in-situ observation. It can be noted that the IF-B model is able to better simulate the damages experienced by the collapsed building.

6.2 Pushover analysis

Displacement-controlled pushover analyses were performed on both the principal directions of the building, x and z, with the purpose of evaluating the mechanisms of failure for the different models. For the sake of conciseness, the following discussion focuses on the results related to the pushover analyses in the x-direction. Similar behavior was observed from the analysis along z-direction. A comparison between the response of the Bare frame and the IF-B illustrates the influence of the exterior infills. The results of the analyses are schematically illustrated by the pushover curves, in terms of base shear vs. roof drift (i.e. the drift of the master node at the roof level). Critical points on the pushover curves are defined as follows:

- Point A (V_A, D_A): indicates the base shear and roof drift at the initial cracking of the infills;
- Point B (V_B, D_B): indicates the base shear and roof drift at the first failure of the infill (where failure occurs when the strut reaches its axial compression strength);
- Point C (V_C, D_C): indicates the base shear and roof drift at the peak strength of the building;

- Point D (V_D , D_D): indicates the base shear and drift corresponding to the shear failure of last lateral resisting elements that failed.

Table 8 provides values of the critical points (k_{in} indicates the initial stiffness of the building measured at a value of base shear equal to 10% of the V_p), while Fig. 16 provides the pushover curves for the BF, IF-B, and IF-D models.

6.3 Bare frame vs. IF-B response

As well known since the 1970s (Mainstone 1971, Bertero *et al.* 1983) the presence of infills strongly affects the global behavior of the building in terms of strength, displacement and global ductility. Inspection of the pushover curves for the BF and IFB models highlights that:

- the initial stiffness increases by an order of magnitude;
- the peak strength capacity increases by a factor equal to 55% of bare frame strength;
- displacement capacity at peak strength reduces by 50% of that of the bare frame.

Table 9 identifies the progression of significant failure events (indicated also in the pushover curve of Fig. 16) that cause the failure of the lateral resisting system for the IF-B model. For each event is indicated base shear, roof drift and a description of the element (or elements) that collapsed. All failures are concentrated at the bottom story indicating a soft/weak story mechanism at the ground floor.

Table 8 Base shear (V) roof drift (D) of the significant point and initial stiffness (k_{in}) from the pushover curves

Point	Bare		IF-B		IF-D	
	V [kN]	D [%]	V [kN]	D [%]	V [kN]	D [%]
A	/	/	3300	0.04	3300	0.04
B	/	/	5100	0.20	5100	0.20
C	3500	0.73	5470	0.33	5485	0.44
D	2340	0.73	2850	0.50	2760	0.56
K_{in}	70000 kN/m		950000 kN/m		950000 kN/m	

Table 9 Numerical values of base shear and roof drift of the main failure events for the IF-B model

Event number	V_{base} [kN]	D [%]	Failure
B1	5160	0.20	Shear failure of 1 st story infills
B2	5470	0.33	Shear failure of 1 st story columns
B3	5080	0.35	Shear failure of 1 st story columns
B4	4200	0.38	Shear failure of 1 st story columns
B5	3380	0.43	Shear failure of 1 st story infills /columns
B6	3090	0.49	Shear failure of infills /columns
B7	2760	0.50	Shear failure of 1 st story infills

6.4 IF-B vs. IF-D response

Fig. 16 compares the response of the two models for the infilled frame. It can be first noticed that both models have a similar global mechanism of failure: a progressive failure of infills and columns producing a soft/weak story mechanism at the ground floor. However, although the global strength capacity of the structures is the same for both the models, the IF-D response exhibits an increase of 7% more strength and 14% less displacement. The higher performance of IF-D model results from a different sequence of failures relative to the IF-B models due to the more ductile shear elements. For the IF-B model, the failure of the infill at the 1st story is observed prior to column shear failure. The IF-D model shows infill failure also at the upper stories before the column shear failure at the 1st story.

Table 10 gives a summary of the sequence of main failure event (vertical drop in the push over curve).

Table 10 Numerical values of base shear and roof drift of each failure events for the IF-D model

Event number	V [kN]	D [%]	Failure
D1	5160	0.20	Infills @ bottom
D2	5820	0.43	Infills @ upper stories
D3	5110	0.50	Infills @ upper stories
D4	4530	0.52	Infills /Columns @ bottom
D5	3290	0.55	Infills /Columns @ bottom
D6	2760	0.58	Infills /Columns @ bottom

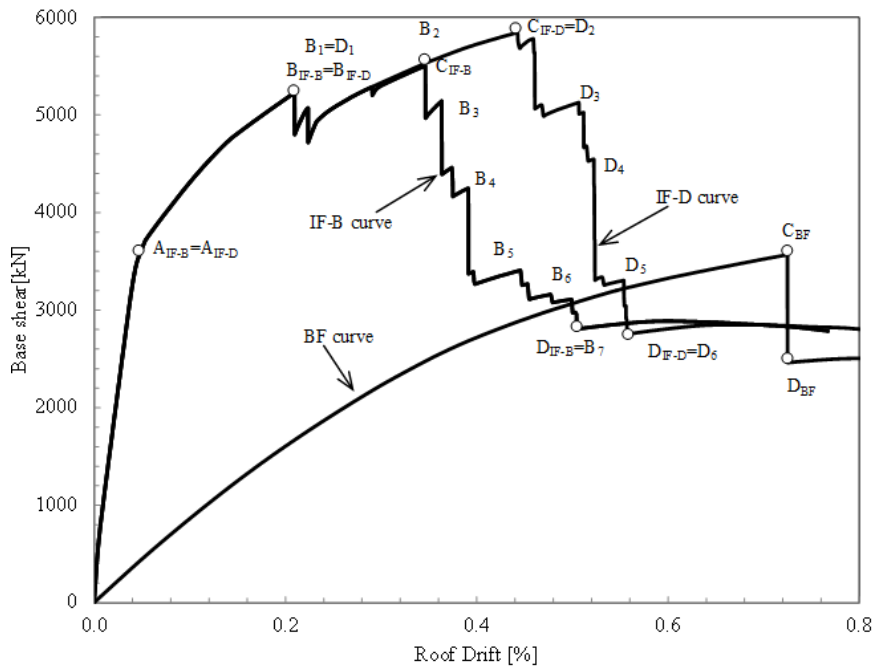


Fig. 16 Pushover curves for BF, IF-B and IF-D models

6.5 Incremental Dynamic Analysis (IDA)

Incremental Dynamic Analyses (IDAs) have been developed according to Vamvatisikos and Cornell 2002 aimed at comparing the estimated value of PGA leading to significant building damage relative to the estimated PGA at the site. Each model (i.e. BF, IF-B and IF-D) was subjected to selected ground motions that were scaled to varying intensity levels (IM), thus producing, for each ground motion, a response curve parameterized versus intensity level. The intensity levels, expressed in terms of PGA, vary between 0.10 and 1.10 g. The adopted Damage Measure (DM) variable is the peak roof drift. Based on the results of the push-over analysis reported in the previous section, the following four Damage Levels (DL), corresponding to the Fully Operational limit state (DL_A), the Operational limit state (DL_B), the Life Safe limit state (DL_C) and the Near Collapse limit state (DL_D), have been adopted:

- DL_A is achieved at a peak roof drift corresponding to point A on the pushover curve;
- DL_B is achieved at a peak roof displacement corresponding to point B on the pushover curve;
- DL_C is achieved at a peak roof displacement corresponding point C on the pushover curve;
- DL_D is achieved at a peak roof displacement corresponding to the point D on the pushover curve;

The values of DL adopted for the different models are summarized in Table 11. Only the DL_C and DL_D have been considered for the BF model.

Table 11 Values of DL adopted for the three models, based on the pushover responses, expressed in terms of roof drift (%)

Model	DL_A	DL_B	DL_C	DL_D
BF	/	/	0.73	0.73
IF-B	0.04	0.20	0.33	0.50
IF-D	0.04	0.20	0.44	0.56

The response of each Single-Record IDA study (Vamvatisikos and Cornell 2002) is a curve (IDA curve) which plots DM versus IM . For sake of conciseness only the IDA curves related to the AQV records are discussed. Similar results are observed for the other ground motions. Table 12 gives a summary of the PGA corresponding to the damage levels DL_C and DL_D that provides an estimation of the PGA that causes the column shear failure of the lateral resisting elements of the three models.

Table 12 Values of PGA corresponding to the damage levels obtained from the IDA analysis

Model	DL_C	DL_D
BF	0.38g	0.38g
IF-B	0.62g	0.82g
IF-D	0.78g	0.90g

6.6 IDA curve for bare frame model

The IDA curve for the BF model is plotted in Fig. 17(a). The curve (as well as Table 12) shows that the BF model reaches the damage levels DL_C and DL_D for a PGA less than 0.40 g. This is an expected behavior for a reinforced concrete building designed prior to modern day seismic requirements.

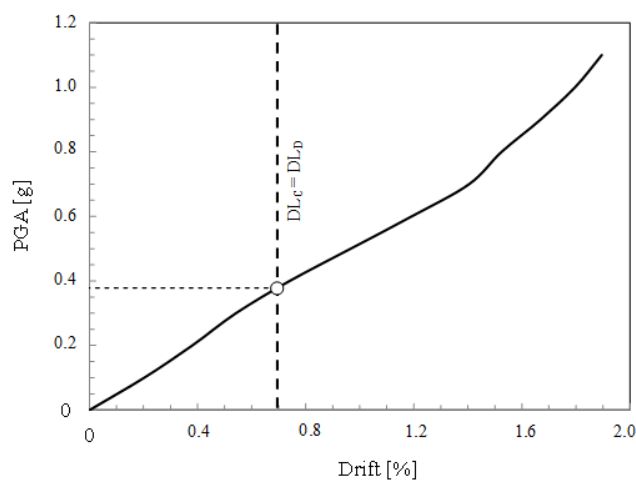
6.7 IDA curve for IF-B model

The IDA curve for IF-B model is plotted in Fig. 17(b). Inspection of the graphs reveals that:

- The first damage level (DL_A), corresponding to the failure of the first infill is reached for a PGA approximately equal to 0.18 g. This indicates that the exterior infills are able to remain in the elastic range up to a level of PGA corresponding to a design PGA which is typical for a low seismic region.
- The second limit state (DL_B) is achieved at a PGA approximately equal to 0.50 g, that is higher than the actual design PGA for common building adopted in Italy (i.e. an earthquake with a return period equal to 476 years).
- The third and fourth damage levels are achieved at a PGA approximately equal to 0.60 g and 0.80 g. In other words according to the IF-B model the building should collapse for a PGA between 0.6 g and 0.8 g. This result is an agreement with the value of PGA that has been estimated at the site of the collapsed building.

6.8 IDA curve for IF-D model

The IDA curve for the IF-D model is graphically represented in Fig. 17(c). Inspection of the graph reveals that:



(a)

Continued

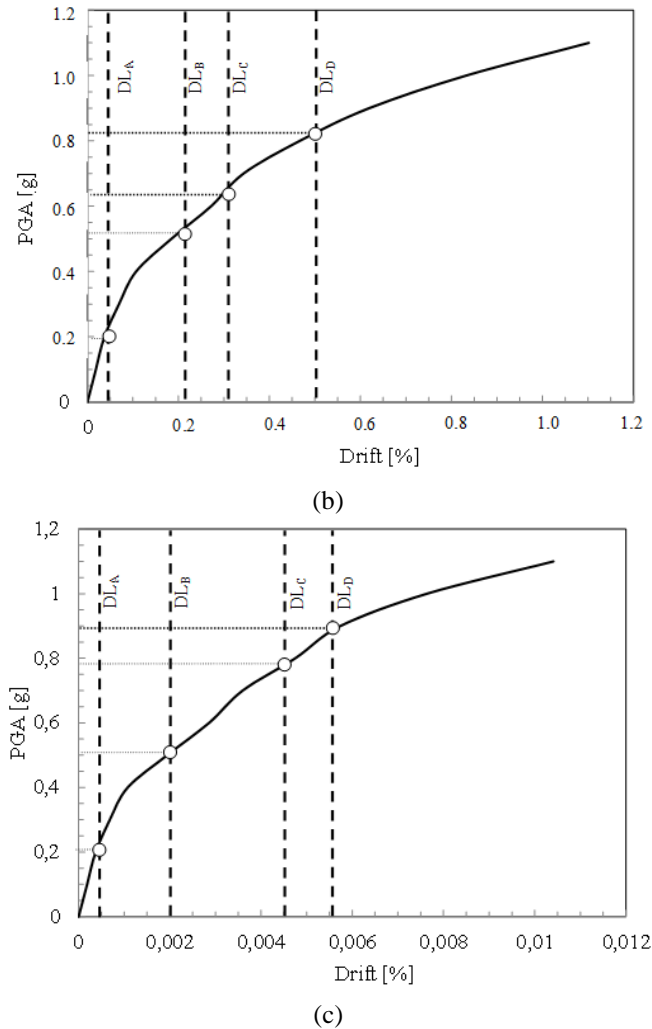


Fig. 17 IDA curves for: (a) BF model, (b) IF-B model and (c) IF-D model

- The first two damage levels (DL_A and DL_B) are reached at the same PGA of model IF-B. This is an expected behavior because the columns are within the elastic range;
- The third and fourth damage levels are achieved at a PGA equal approximately to 0.80 g and 0.90 g, respectively. This result confirms the significant influence of ductile detailing on the seismic response of the building. Furthermore it can suggest a preliminary possible explanation of the different behavior observed for the other similar buildings at the site that did not collapse: the presence of possibly more ductile column detailing may have prevented the collapse of the other buildings.

A more complete study, aimed at investigating in more detail the effects of the different column details through additional in-situ survey and the research of the original plans for all the seven

buildings, as well a more in-depth study of possible different soil amplification effects related to the specific characteristic of the soil of each building site, is required.

7. Conclusions

This paper presents the results of a research work focused on the study of the seismic response of seven similar buildings located in L'Aquila, two of which collapsed during the recent 2009 L'Aquila, Italy earthquake, that arose a great interest among the earthquake engineering community. The main purpose of the research is to investigate the reasons the different seismic behavior. The present paper is mainly focused on the study of one of the two collapsed buildings with the purpose of determining the reliability of state-of-the practice techniques to predict the observed behavior of the building. Based on this case study, we can make the following conclusions:

1. The estimated peak ground at the site, based on the application of currently accepted attenuation relationships, along with consideration of the effects soil amplification, was approximately 0.70g (note that this value of ground acceleration is quite larger than the current design acceleration for a reinforced concrete building located in an high seismicity region in Italy, approximately equal to 0.50 g considering the maximum soil amplification factor as per Italian building code). The high value of PGA at the site of the studied building is mainly due to a local soil amplification effect due to the presence of a soft alluvial layer of soil (as documented from the INGV investigation leading to the microzonation map of the L'Aquila region).
2. Based on incremental dynamic analyses with a Brittle model (representative of a nonductile shear-controlled column with poor confinement detailing), based on the in-situ measured details on the collapsed building, we could have predicted that the building reached the Near Collapse limit state at a peak ground acceleration of 0.60g. On the contrary performing the incremental dynamic analyses with a Semi-ductile model (representative of a less nonductile shear-controlled column with slightly better confinement detailing), we would have predicted that the building reached the Near Collapse limit state at a PGA between 0.80 g and 0.90 g, thus greater than the estimated PGA at the site of the building. Therefore, it is likely that the buildings that collapsed had poorer confinement detailing relative to the buildings that did not collapse.
3. As a further confirmation of the previous observation, the results of time history analysis performed using the recorded accelerograms scaled at the PGA experienced by the building highlighted that: (i) the Brittle model showed a mechanism of failure characterized by a severe torsional response that caused shear failure at select perimeter infill walls followed by column shear failure ending in collapse; (ii) on the contrary, the Semi-ductile model showed a mechanism of damage at the exterior infills without the shear failure of the columns.
4. Pushover analyses (as well as incremental dynamic analysis) has been useful in order to confirm two aspects already well known in literature:
 - i. Infill panels influence stiffness, strength and global ductility of the building and should not be neglected in the evaluation and retrofit of these types of buildings. As such, an asymmetrical distribution of infill walls will result in a torsional effect that will have an adverse effect on the bare frame response. In detail, for the studied building the overall effect of the infills may be considered as positive provided that it led to a not negligible increase of the strength capacity of the building, if compared to the bare structure which

- most probably should have collapsed for a much lower seismic intensity; however, the asymmetric collapse of the perimeter infills most probably contributed to the observed weak/soft story mechanism of collapse.
- ii. In the case of light reinforced columns, a slight variation in columns details (e.g. deformed transverse ties versus smooth bars, 90° or 135° hooks, etc.) or also the level of axial load acting during the earthquake will significantly affect the seismic response of the building.
5. Using the most current analysis techniques readily available to the design professional (i.e. a non-linear diagonal strut model for the exterior infills and an appropriate backbone curve for columns shear failure), we were able to predict the building performance that correlated to the observed building damage. Especially noteworthy to the reader is the fact that care should be taken to use the correct shear failure model (i.e. Brittle or Semi-ductile) to correctly predict building behavior.

References

- Al-Chaar, G. (2002), "Evaluating strength and stiffness of unreinforced masonry infill structures", *ERDC/CERL TR-02-1, US Army Corps of Engineers, Engineer Research Development Center, Vicksburg, Miss.*
- ASCE/SEI 41 (2007), *Seismic rehabilitation of existing buildings*, American Society of Civil Engineers, Reston, Virginia.
- Bertero, V.V. and Brokken, S. (1983), "Infills in seismic resistant building", *J. Struct. Eng.*, **109**(6), 1337-1361.
- Bursi, O.S. (2009), "A reconnaissance report", The April 6, L'Aquila Earthquake, Italy, available on <http://www.reluis.it>.
- Chioccarelli, E., De Luca, F. and Iervolino, I. (2009), "Preliminary study on L'Aquila earthquake ground motion records V5.2", available on <http://www.reluis.it>.
- Chioccarelli, E. and Iervolino, I. (2009) "Direttività e azione sismica: discussione per l'evento de L'Aquila", available on <http://www.reluis.it>.
- Chopra, A.K. and Goel, R.K. (2002), "A modal pushover analysis procedure for estimating seismic demands for buildings", *Earthq. Eng. Struct. Dyn.*, **31**,561-582.
- Colangelo, F. (2005), "Pseudo-dynamic seismic response of reinforced concrete frames infilled with non-structural brick masonry", *Earthq. Eng. Struct. Dyn.*, **34**, 1219-1241.
- De Stefano, M., Tanganelli, M. and Viti, S. (2013), "On the variability of concrete strength as a source of irregularity in elevation for existing RC buildings: a case study", *Bull. Earthq. Eng.*, **11**(5), 1711-1726.
- Decreto Ministeriale 26-03-1980 (1980), *Norme tecniche per l'esecuzione delle opere in cemento armato normale, precompresso e per le strutture metalliche*, Gazzetta Ufficiale 28-06-1980 n.176. (in Italian)
- Decreto Ministeriale 3-03-1975 N. 40 (1975), *Disposizioni concernenti l'applicazione delle norme tecniche per le costruzioni in zone sismiche*, Gazzetta Ufficiale 8-4-1975, n. 93 - suppl, Italy. (in Italian)
- Earthquake Engineering Research Institute EERI (2009), "Learning from Earthquakes", The Mw 6.3 Abruzzo, Italy, earthquake of April 6, 2009, EERI Special Earthquake Rep., Oakland, Calif available on <http://www.reluis.it>.
- Elwood, K. and Moehle, J. (2005), "Drift capacity of reinforced concrete columns with light transverse reinforcement", *Earthq. Spectra*, **21**(1), 71-89.
- Fib Bulletin 24 (2003), *Seismic assessment and retrofit of reinforced concrete buildings*, International Federation du Beton, Lausanne, Switzerland.
- Galli, P. and Camassi, R. (2009), "Rapporto sugli effetti del terremoto aquilano del 6 aprile 2009", *Rapporto congiunto DPC-INGV*, 12 pp. available on <http://www.reluis.it>.

- Haselton, C.B., Goulet, C., Mitrani-Reiser, J., Beck, J., Deierlein, G.G., Porter, K.A., Stewart, J.P. and Taciroglu, E. (2007), "An assessment to benchmark the seismic performance of a code-conforming reinforced-concrete moment-frame building", PEER Report 2007, University of California, Berkeley, CA. <http://www.protezionecivile.gov.it>
- Iervolino, I. and Chioccarelli, E. (2010), "Near-source seismic demand and pulse-like records: a discussion for L'Aquila earthquake", *Earthq. Eng. Struct. Dyn.*, **39**, 1039-1062.
- Mainstone, R.J. (1971), "On the stiffnesses and strengths of infilled frames", *Proc., Instn. Civ. Engrs., Supp.* (iv), 57-90.
- Manfredi, G., Masi, A., Pinho, R., Verderame, G. And Vona, M. (2007), *Valutazione degli edifici esistenti in Cemento Armato*, IUSS Press, Pavia, Italy. (in Italian)
- Mausi, A. and Chiausi, L. (2009), "Preliminary analysis on the mainshock of the L'Aquilano earthquake occurred on April 06 2009", available on <http://www.reluis.it>.
- Mazzoni, S., McKenna, F. and Fenves, G.L. (2006), *Open system for earthquake engineering simulation user manual*, Pacific Earthquake Engineering Research Center, University of California, Berkeley, available on <http://opensees.berkeley.edu/>.
- Sabetta, F. and Pugliese, A. (1996), "Estimation of response spectra and simulation of nonstationarity earthquake ground motions", *Bull. Seismal. Soc. Am.*, **86**, 337-352.
- Tanganelli, M., Viti, S., De Stefano, M. and Reinhorn, A.M. (2013), "Influence of infill panels on the seismic response of existing RC buildings: a case study", *In: M. De Stefano, O. Lavan. Seismic behaviour and design of irregular and complex civil structures*, 119-133, Dordrecht, Heidelberg, New York, London, Springer.
- Vamvatisikos, D. and Cornell, C.A. (2002), "Incremental dynamic analysis", *Earthq. Eng. Struct. Dyn.*, **31**, 491-514.
- Verderame, G.M., Iervolino, I. and Ricci, P. (2009), "Report on the damages on buildings following the seismic event of 6th of april 2009", V1.20 available on <http://www.reluis.it>.